

The anticenter old open cluster NGC 1883: radial velocity and metallicity

Sandro Villanova¹, Gustavo Baume², Giovanni Carraro¹ \star

¹*Dipartimento di Astronomia, Università di Padova, vic. Osservatorio 3, Padova, Italy*

²*Facultad de Ciencias Astronómicas y Geofísicas de la UNLP, IALP-CONICET, Paseo del Bosque s/n, La Plata, Argentina*

Submitted: —

ABSTRACT

Having already reported on the first photometric study of the intermediate-age open cluster NGC 1883 (Carraro et al. 2003), we present in this paper the first spectroscopic multi-epoch investigation of a sample of evolved stars in the same cluster. The aim is to derive the cluster membership, velocity and metallicity, and discuss recent claims in the literature (Tadross 2005) that NGC 1883 is as metal poor as globular clusters in the Halo. Besides, being one of the few outer Galactic disk intermediate-age open clusters known so far, it is an ideal target to improve our knowledge of the Galactic disk radial abundance gradient, that is a basic ingredient for any chemical evolution model of the Milky Way. The new data we obtained allow us to put NGC 1883's basic parameters more reliable. We find that the cluster has a mean metallicity of $[\text{Fe}/\text{H}] = -0.20 \pm 0.22$, from which we infer an age (650^{+70}_{-70} Myr) close to the Hyades one and a Galactocentric distance of $12.3^{+0.4}_{-0.2}$ kpc. The metal abundance, kinematics, and position make NGC 1883 a genuine outer disk intermediate-age open cluster. We confirm that in the outer Galactic disk the abundance gradient is shallower than in the solar vicinity.

Key words: Open clusters and associations: general– Open clusters and associations: individual: NGC1883– Milky Way: structure and evolution

1 INTRODUCTION

NGC 1883 is a northern open cluster, located in the second Galactic quadrant, toward the anticenter direction ($\alpha = 05^h 25^m.9$, $\delta = +46^\circ 29'$, $l = 163^\circ.08$, $b = +06^\circ.16$, $J2000.0$). This cluster was studied by Carraro et al. (2003, hereafter C03), who present the first BVI CCD photometric observations suggesting an age of about 1 Gyr and a distance of 4.8 kpc from the Sun.

This would imply a Galactocentric distance larger than 13 kpc, and would make NGC 1883 a key object for our understanding of the properties of the outer Galactic disk. However, both age and distance are uncertain because of the unknown metallicity of the cluster.

At the position of NGC 1883 the mean abundance (Friel 1995) should be significantly lower than solar. Unfortunately, the exact amount of this under-abundance is poorly constrained, also in light of the results by Twarog et al. (1997), Carraro et al. (2004), and Yong et al. (2005), that

suggest that the disk abundance gradient for Galactocentric distances larger than ~ 10 kpc gets much shallower than in the solar vicinity.

Using solar metallicity ($Z=0.019$) C03 estimated $E(B-V)=0.23$, $(m-M)_V=14.00$ for NGC 1883, and $E(B-V)=0.35$, $(m-M)_V=14.50$ adopting a lower metal content ($Z=0.008$), which by the way seems to provide a better fit to the star distribution in the Colour Magnitude Diagram (CMD).

A more recent study was performed by Tadross (2005, hereafter T05) using C03 BVI data and JHK 2MASS data.

This author obtained a photometric metallicity of about $[\text{Fe}/\text{H}]\sim -1.1$ ($Z\sim 0.0015$), much lower than that estimated by C03, and closer to globular clusters. The disagreement between the two abundance estimations has to be solved in order to obtain reliable parameters for this cluster. In fact, NGC 1883 is one of the few intermediate-age open clusters located in the outer Galactic disk. For this reason, it plays an important role in defining the shape of the radial abundance gradient in the external regions of the Galactic disk, which is one of the fundamental constraints of models of chemical evolution (Cescutti et al. 2007).

For this purpose, this paper presents the first spectroscopic study of the cluster aiming at finding the member stars

\star email:

sandro.villanova@unipd.it (I), gbaume@fcaglp.fcaglp.unlp.edu.ar (Ar), giovanni.carraro@unipd.it (I)

from radial velocity measurements, and to estimate a reliable value for the metallicity. Section 2 of this paper illustrates the observation and reduction strategies. In Section 3 and 4 we discuss the membership and the abundance determination. Section 5 is devoted to a comparison between this paper and previous ones. Section 6 deals with a new determination of cluster reddening, distance and age. Section 7 compares the observed CMD with a synthetic one. Section 8 and 9 are devoted to the determination of structural parameters for the cluster (radial profile, luminosity function, and mass function). Finally Section 10 discusses NGC1833 in the context of the Galactic abundance gradient.

2 OBSERVATIONS AND DATA REDUCTION

Medium-high resolution ($R \approx 20000$) spectra of 5 candidate evolved stars in the field of NGC1883 have been obtained using the REOSC Echelle Spectrograph on board of the 1.82 m telescope of Asiago Astronomical Observatory. The Echelle spectrograph works with a Thomson 1024 \times 1024 CCD and the wavelength coverage for our observations is approximately 4600-6400 Å. Details on this instrument are given in the Asiago Observatory Home page (www.oapd.inaf.it/asiago/).

The exposures were 3×15 min for all stars. To improve the signal to noise ratio the three exposures were added reaching S/N values up to 20. Each star was observed during three epochs, December 2004 (A), January 2005 (B), January 2006 (C), allowing us to establish the binarity of each target.

Data were reduced with the IRAF package[†], including bias subtraction, flat-field correction, frame combination, extraction of spectral orders, wavelength calibration, sky subtraction, and spectral normalization. By comparing known sky lines positions along the spectra we obtained an error in wavelength calibration of less than 0.01 Å (< 0.5 km/s).

Details of the observed stars are listed in Table 1, while the positions of these targets on CMDs are plotted in Fig. 1. The first column of Tab. 1 gives the ID number of the star according to USNO-2.0 catalogue, the second and third the coordinates, the fourth, fifth, sixth, and seventh the V magnitude and B-V, V-I, V-K colours, the eighth, ninth, and tenth columns the measured radial velocity at different epochs expressed in km/s.

The photometry for our stars was taken from C03 (B,V,I magnitudes), and from 2MASS (K magnitude).

Radial velocity was measured using the IRAF package FXCOR, which cross-correlates the observed spectrum with a template. As a template we used a synthetic spectrum having mean atmospheric parameters close to the cluster RGB stars ($T_{\text{eff}}=4500$ K, $\log(g)=3.0$, $[\text{Fe}/\text{H}]=0.0$, $v_t=1.5$ km/s). Finally the heliocentric correction was applied. The typical error for our measurements is less than 1 km/s.

[†] IRAF is distributed by the National Optical Astronomy Observatory, which is operated by the Association of Universities for Research in Astronomy, Inc., under cooperative agreement with the National Science Foundation.

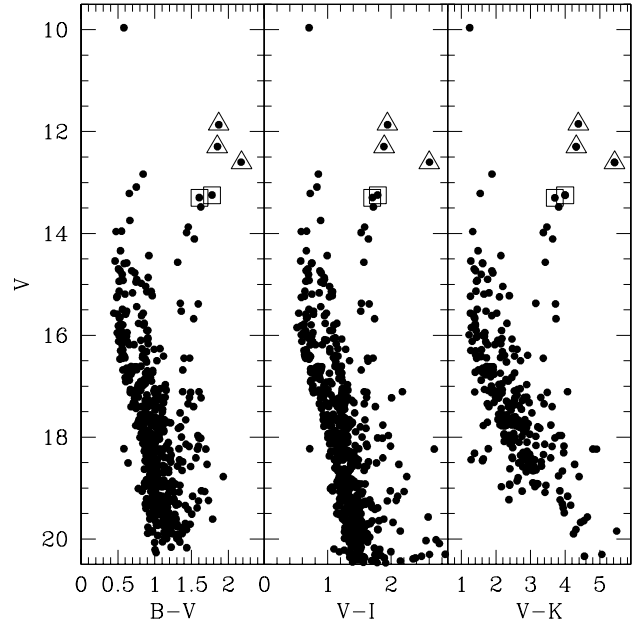


Figure 1. CMD for the stars in the field of NGC 1883. *left:* V vs B-V diagram from C03. *center:* V vs V-I diagram from C03. *right:* V vs V-K diagram (K magnitude from 2MASS). Open squares are member stars (#75374, #76058), while open triangles are background objects. See text for more details.

3 MEMBERSHIP AND CLUSTER MEAN RADIAL VELOCITY

We make use of these radial velocities to establish star membership to NGC 1883. Firstly, we notice that each star has radial velocities constant among the three epochs within the errors. We are led to the conclusion that none of the targets are short-period binaries. The mean radial velocity and membership of all the targets is reported in Tab. 2 where member stars are indicated by M, while non-member by NM. Only #75374 and #76058 stars have compatible radial velocity and therefore we consider them as genuine members (open squares in Fig. 1) of the cluster. The average of the velocities of #75374 and #76058 gives us the mean radial velocity of the cluster:

$$\langle RV_{\text{helio}} \rangle = -30.8 \pm 0.6 \text{ km/s}$$

The members stars will be used in the following Section to obtain the metal content of NGC 1883.

4 ABUNDANCE MEASUREMENTS

The $[\text{Fe}/\text{H}]$ content was obtained from summed spectra of member stars (#75374 and #76058) in a interactive way. The most important parameter for abundance determination is T_{eff} , that for our stars can be obtained from dereddened B-V, V-I, and V-K colours. But the reddenings $E(\text{B}-\text{V})$, $E(\text{V}-\text{I})$, and $E(\text{V}-\text{K})$ for the cluster can be obtained only by isochrones fitting, with isochrones having the cor-

Table 1. Observed stars

ID(U-1350-057...)	R.A.(J2000.0)	Decl.(J2000.0)	V	B-V	V-I	V-K	RV _H (A)	RV _H (B)	RV _H (C)
79024	05:26:02.01	+46:29:26.9	12.30	1.85	1.89	4.32	34.4	33.0	34.4
75374	05:25:51.69	+46:29:35.4	13.25	1.78	1.79	4.00	-29.7	-32.5	-32.1
76058	05:25:53.66	+46:26:20.5	13.30	1.61	1.70	3.70	-29.8	-30.3	-30.7
81797	05:26:09.92	+46:25:55.4	11.85	1.87	1.94	4.38	2.7	3.0	2.7
85248	05:26:19.92	+46:31:41.4	12.61	2.18	2.60	5.43	-17.9	-18.5	-18.4

rect metallicity. For this reason we firstly assumed a solar metallicity for our stars, obtaining a first guess for reddening by isochrones fitting. Then, using the T_{eff} value calculated for this reddening, we measured the metallicity for our stars (see below). Using this metallicity, we obtained a new reddening and a new abundance. This procedure was iterated until convergence was achieved.

T_{eff} was derived from the colour-[Fe/H]-temperature relation from Alonso et al. (1999) using dereddened colours. The gravity was derived from the value given by the isochrones at the given position of the stars in the CMD, while the microturbulent velocity come from the relation (Houdashelt et al. 2000):

$$v_t = 2.22 - 0.322 \times \log(g)$$

The adopted atmospheric parameters for our stars are reported in Table 2, and the typical random errors are 100 K for T_{eff} , 0.2 for $\log(g)$, and 0.2 km/s for v_t .

We derived metallicity from equivalent widths of selected spectral lines. The equivalent width was derived by gaussian fitting of these spectral features. Repeated measurements show a typical error of about 10 mÅ. Because of the low S/N and the resolution of our spectra, we could measure only the strongest Fe lines (~ 10 for each star) in the region $\lambda > 5500$ to avoid crowding. For this reason we give only Fe content of our stars (see Tab. 2). The LTE abundance program MOOG (freely distributed by C. Sneden, University of Texas, Austin; see <http://verdi.as.utexas.edu/>) was used to determine the metal abundances. Model atmospheres were interpolated from the grid of Kurucz (1992) models by using the values of T_{eff} and $\log(g)$ of Tab. 2. The error on measurements is high (0.2-0.4 dex), but a weighted mean of the obtained metallicities gives a good estimation of the iron content:

$$[\text{Fe}/\text{H}] = -0.20 \pm 0.22$$

This value is important for the discussion reported in the following Sections and for the comparison with previous works. The errors for iron content we report here and in Tab. 2 represent only internal random errors, mainly due to the uncertainty in the equivalent width measurements. Systematic errors are more difficult to estimate, and are mainly due to uncertainties in colour- T_{eff} relations and in reddening. The typical systematic error on T_{eff} scale for this temperature range is 100 K giving a systematic uncertainty on metallicity of 0.02 dex.

5 COMPARISON WITH PREVIOUS WORK

Firstly, we compare our results with C03. In that paper the authors estimate a range in metallicity between $Z \sim 0.019$ ($[\text{Fe}/\text{H}] = 0.0$) and $Z \sim 0.008$ ($[\text{Fe}/\text{H}] = -0.41$) by isochrones fitting of the TO. Our measurements lie exactly in the middle confirming those results. On the other hand, our value largely disagrees with T05. This author gives $[\text{Fe}/\text{H}] \sim -1.1$, based on the slope of the RGB stars (Vallenari et al. 2000 and references therein). The method can give a reasonable estimate of the metallicity of a cluster (Tiede et al. 1997), but $[\text{Fe}/\text{H}] \sim -1.1$ is definitely ruled out by our measurements. T05 results can be explained by a poor treatment of stellar contamination. As a matter of fact, background stars always contaminate the field of a cluster, and an identification of the members is needed before applying RGB-slope method. This is the case of NGC 1883, where a fraction of stars that apparently populate the RGB are background objects, as Fig. 1 unambiguously shows. This contamination changes the real slope of the RGB and the $[\text{Fe}/\text{H}]$ estimate by T05 is clearly affected by this problem. As shown in Fig. 1 the RGB slope in T05 is mainly based on #79024, #81797, and #85248 stars (open triangles) that, according to our radial velocities, are not members. This leads us to the conclusion that T05 metallicity is untenable.

6 CLUSTER FUNDAMENTAL PARAMETERS

Having an estimate of the metal content ($[\text{Fe}/\text{H}] = -0.20$), we now provide a more reliable estimate of the cluster parameters. We make use of the comparison between the distribution of the stars in the CMDs presented in C03 and a set of theoretical isochrones from the Padova group (Girardi et al. 2000). In Fig. 2 we superimposed an isochrone with $[\text{Fe}/\text{H}] = -0.20$ ($Z = 0.012$) and an age of 650 Myr. The TO fit is very good both in V vs B-V, V vs V-I, and V vs V-K diagrams, and the shape of the MS is well reproduced. Also the location of #75374 and #76058 stars in the RGB is well matched. By this fitting we obtained $(m-M)_V = 14.30$ and $E(B-V) = 0.43$, $E(V-I) = 0.52$, $E(V-K) = 1.15$.

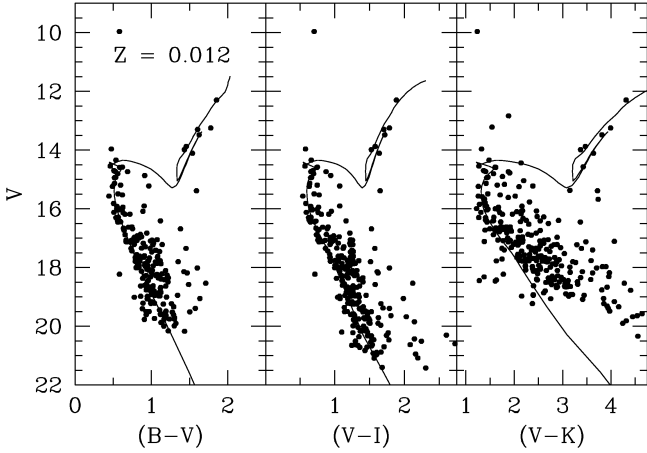
The reddening value we obtained is compatible with Schlegel et al. (1998) maps which, in the direction of NGC 1883, predict a $E(B-V)$ value of 0.55, all the way to infinity.

NGC 1883 turns out to be located 3.9 kpc from the Sun towards the anticenter direction. This yields from the heliocentric rectangular Galactic coordinates $X = -3.71$ kpc, $Y = 1.13$ kpc, $Z = 0.41$ kpc, and a distance from the Galactic center of 12.3 kpc.

The age we found in this study is somewhat smaller (about 350 Myr) than in C03, but NGC 1883 can still be considered

Table 2. Mean radial velocity, membership, and parameters for the observed stars

ID	$\langle RV_H \rangle$ (km/s)	Membership	T_{eff} (K)	$\log(g)$	v_t (km/s)	[Fe/H]
79024	33.9	NM	-	-	-	-
75374	-31.4	M	4172	2.75	1.3	-0.25 ± 0.26
76058	-30.3	M	4462	2.75	1.3	-0.07 ± 0.46
81797	2.8	NM	-	-	-	-
85248	-18.3	NM	-	-	-	-

**Figure 2.** Isochrones fitting of the photometric data using the metallicity obtained in Section 4. *left:* V vs $B-V$ diagram from C03. *center:* V vs $V-I$ diagram from C03. *right:* V vs $V-K$ diagram (K magnitude from 2MASS). See text for more details.

one of the few intermediate-age open cluster located in the outer Galactic disk.

The distance estimate is also confirmed by the V magnitude of the red-clump stars (Girardi & Salaris 2001). They are identified with the group of three stars having $\langle V \rangle = 14.0$ and $\langle B-V \rangle = 1.45$ (see Fig. 2). A V magnitude of 14.0 for red-clump stars gives a distance of 3.6 ± 0.4 kpc from the Sun, that agrees well with the value we obtained with isochrone fitting.

We interpret the two member stars at V 13.3 as bright RGB stars. In fact, the interpretation of these two stars as clump stars would imply a magnitude difference between clump and TO $\Delta V = 2.1$, and, in turn, an age larger than 3 Gyr (Carraro & Chiosi 1994). An isochrone for this combination of age and metallicity would have too a blue clump, and produce a serious mismatch of the evolved stars distribution. Besides, it would imply a reddening close to zero ($E(B-V) \sim 0.06$), too small for a cluster which in this case would lie at 1.7 kpc from the Sun.

7 SYNTHETIC CMDs

To better establish the basic parameters of the cluster we calculated synthetic V vs $B-V$ CMDs. We started from the Girardi et al. (2000) theoretical isochrone of metallicity $Z = 0.012$ used for our previous fitting. The isochrone was shifted in apparent magnitude and colour of the amount found in the last Section. The sequence of steps required to

simulate a CMD aimed to reproduce the NGC 1883 data are:

- The 650 Myr old isochrone of $Z = 0.012$ is used to simulate a cluster with 3 red clump stars (see previous Section). Assuming a Kroupa (2001) IMF, in order to reach this number we need an initial cluster mass of about $8.0 \times 10^2 M_\odot$, which is assumed herein-after. According to the same IMF, we would expect 9-11 stars located beyond the subgiant branch region all the way to the asymptotic giant branch (AGB) region. The exact number and distribution of these stars depend on the simulation *seed*. Anyhow, this range of number matches the observations. In fact (see Fig. 2), despite the fact that always some contamination is expected, we count 7 ± 3 evolved stars, taking into account Poisson uncertainties.

We have simulated detached binaries, assuming that 30 percent of the observed objects are binaries with a mass ratio between 0.7 and 1.0. This prescription is in agreement with several estimates for galactic open clusters (Phelps & Janes 1994) and with the observational data for NGC 1818 and NGC 1866 in the LMC (Elson et al. 1998; Barmina et al. 2002). The result of such simulation is shown in Fig. 3(a). In this panel we can see that most of the stars – the single ones – distribute along the very thin sequence defined by the theoretical isochrone. Binaries appear as both (i) a sequence of objects roughly parallel to the main sequence of single stars, and (ii) some more scattered objects in the evolved part of the CMD.

- In order to estimate the location of foreground and background stars, we use the TRILEGAL[‡] Galaxy model code (Girardi et al. 2005). It includes the several Galactic components – thin and thick disk, halo, and an extinction layer – adopting geometric parameters as calibrated by Groenewegen et al. (2001) (for other applications see Baume et al. 2007, Carraro et al. 2006). The most relevant component in this case is the thin disk, which is modelled by exponential density distributions in both vertical and radial directions. The radial scale height is kept fixed (2.8 kpc), whereas the vertical scale height h_z increases with the stellar age t as

$$h_z = z_0(1 + t/t_0)^\alpha$$

with $z_0 = 95$ pc, $t_0 = 4.4$ Gyr, $\alpha = 1.66$. The simulated field has the same area (8.1×8.1 arcmin²) and galactic coordinates ($\ell = 163^\circ.08$, $b = +6^\circ.16$) as the observed one for NGC 1883. The results are shown in Fig. 3(b). It is noteworthy that, in this direction, most of the Galactic field stars appear in a sort of diagonal sequence in the CMD.

[‡] <http://trilegal.ster.kuleuven.be/cgi-bin/trilegal>

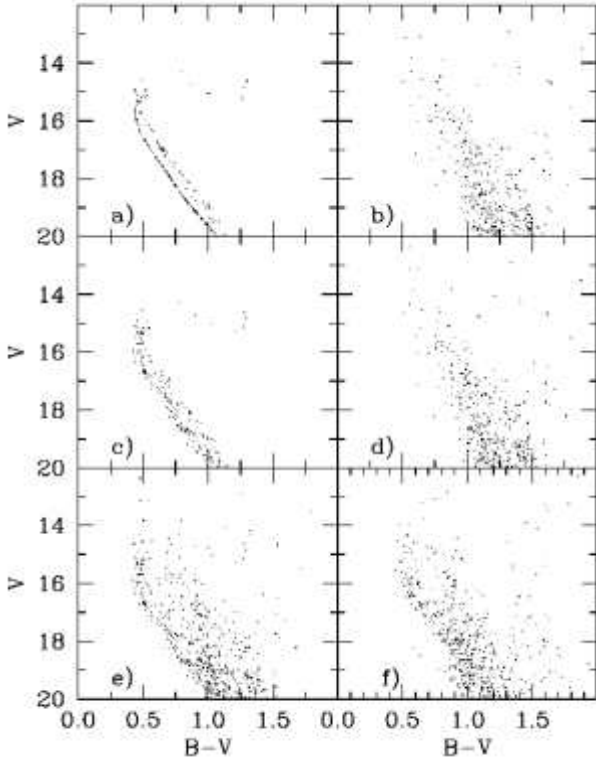


Figure 3. Synthetic CMD diagram for NGC 1883. Panel a) and b): simulated CMDs for the cluster and the field. Panel c) and d): simulated CMDs for the cluster and the field with photometric errors. Panel e): final simulated CMD (cluster+field). Panel f): the observed CMD.

- Within TRILEGAL, there are various options to take reddening into account (Girardi et al. 2005). In the particular case of the simulation we are presenting here, we adopt an exponential dependence of reddening with distance, calibrated at infinity with Schlegel et al. (1998) maps, which provide the reddening along a line of sight all the way to infinity.

- We then simulate the photometric errors as a function of V magnitude, with typical values derived from our observations. The results are shown separately for cluster and field stars in panels (c) and (d) of Fig. 3.

- The sum of field and cluster simulations is shown in Fig. 3(e). This can be compared directly to the observed data shown in Fig. 3(f).

The comparison of these two latter panels indicates that the selected cluster parameters – age, metallicity, mass, distance, reddening, and binary fraction – really lead to an excellent description of the observed CMD, when coupled with the simulated Galactic field. The most noteworthy aspects in this comparison are the location and shape of the turn-off and subgiant branch, that are the features most sensitive to the cluster age.

Of course, there are minor discrepancies between the observed and simulated data, namely: (i) The simulated cluster is better delineated in the CMD than the data. This may be ascribed to a possible underestimate of the photometric errors in our simulations, and to the possible presence of differential reddening across the cluster (ii) There is a deficit

of simulated field stars, that can be noticed more clearly for $V < 16$ and $(B - V) < 1$. This is caused by the simplified way in which the thin disk is included in the Galactic model: it is represented by means of simple exponentially-decreasing stellar densities in both radial and vertical directions, and does not include features such as spiral arms, intervening clusters, etc., that are necessary to correctly describe fields at low galactic latitudes. Anyway, the foreground/background simulation we present is only meant to give us an idea of the expected location of field stars in the CMD.

Although these shortcomings in our simulations might probably be eliminated with the use of slightly different prescriptions, they do not affect our main results, that regard the choice of cluster parameters. Then, we conclude that $(m-M)_V = 14.3$, $E_{B-V} = 0.43$, 650 Myr, $Z = 0.012$ ($[Fe/H] = -0.20$) well represent the cluster parameters. All these values are uncertain to some extent:

- From isochrones fitting we can estimate a maximum error of 10 percent (70 Myr) in the age. One should keep in mind, however, that the absolute age value we derived depends on the choice of evolutionary models, and specially on the prescription for the extent of convective cores. For the stellar masses involved ($M_{TO} \sim 1.8 M_{\odot}$ for NGC 1883), our models (Girardi et al. 2000) include a moderate amount of core overshooting.

- Our best fit model corresponds to $E(B-V)=0.43$ and $(m-M)_V=14.30$, but typical errors for both measurements can reach 10-15%.

- The initial mass estimate depends heavily on the choice of IMF, that determines the mass fraction locked into low-mass (unobserved) objects. The value of $8.0 \times 10^2 M_{\odot}$ was obtained with a Kroupa (2001) IMF, corrected in the lowest mass interval according to Chabrier (2001; details are given in Groenewegen et al. 2001), and should be considered just as a first guess. At present ages, supernovae explosions, stellar mass loss, and tidal effects (Lamers et al. 2005) would have reduced this mass by about 40 percent.

8 SURFACE DENSITY PROFILE

According to C03 and Dias et al. (2002), NGC 1883 has a radius of 2.5-3.0 arcmin. This is the distance from the cluster center where star counts remain flat, reaching the level of the Galactic field. However, to provide more physical quantities, we perform here a comparison with King (1962) models (Fig. 4).

To this aim we first adopt a new cluster center based on the stellar concentration. C03 chose star #12 as center (see Fig. 5), but a more detailed inspection of the cluster appearance suggests that a more appropriate option for the center is $X = 495$, $Y = 605$ pixels (see Fig. 5), which in turns is ($\alpha_{2000} = 05^h 25^m 58^s$; $\delta_{2000} = +46^{\circ} 29' 03''$).

By adopting the new cluster center, we counted the number of stars as a function of the distance from the center, and correct these counts by background contamination. The choice of the background is illustrated in Fig. 5, and implies that one can expect to encounter ~ 4.5 stars/arcmin² in the direction of NGC 1883 down to $V \sim 20$. This value is in reasonable agreement with the predictions of the TRILEGAL model (Section 7), according to which we expect to find 5.2

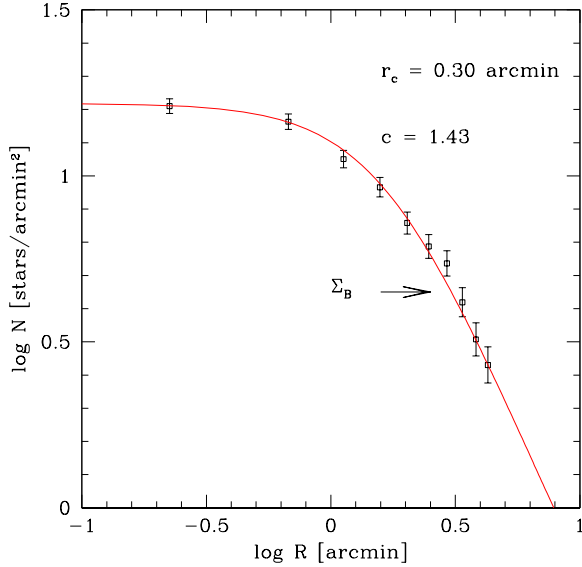


Figure 4. Surface density profile for the cluster. The solid line is a King model for the indicated parameters. Σ_B shows the level of the field background.

stars/arcmin² towards at (l=163.1, b=+6.2).

In Fig. 4 we show star counts together with their Poisson uncertainties. The solid line is the best-fit King profile, which yields a core radius $r_c = 0.30$ arcmin and a concentration $c = \log(\frac{r_t}{r_c}) = 1.43$, where r_t is the cluster tidal radius. r_t results 8.1 arcmin, much larger than the region covered by our photometry. These values can be compared with the recent study by Piskunov et al. (2007), where the authors study the r_c and r_t distribution of a sample of open clusters in the Sun vicinity. According to this study, the open clusters mean c value is ~ 0.6 . Therefore, NGC 1883 looks like a poorly concentrated cluster, on the verge of dissolving into the Galactic disk general field.

9 CLUSTER LUMINOSITY AND MASS FUNCTION

With the aim of deriving an estimate of NGC 1883 integrated luminosity and mass, we construct the luminosity function (LF) of the cluster.

As a first step, we considered the *Cluster Region* and the *Comparison Field*: the first one is a circle centered in the adopted cluster center and 2'.5 in radius; and the later is a region limited for a circle of 3'.11 in radius and a 7'.1 \times 7'.1 square (see Fig. 5). Both regions were chosen to cover the same area.

We estimated then the completeness of our data as in Baume et al. (2004) and assume that it is the same across the whole region. This seems to be a good approximation, provided the cluster is not very crowded. The completeness as a function of magnitude V is given in Table 3

Besides, we assume that our comparison field provides a good estimate of the contamination by field interlopers and is valid across all the cluster surface. The results are plotted

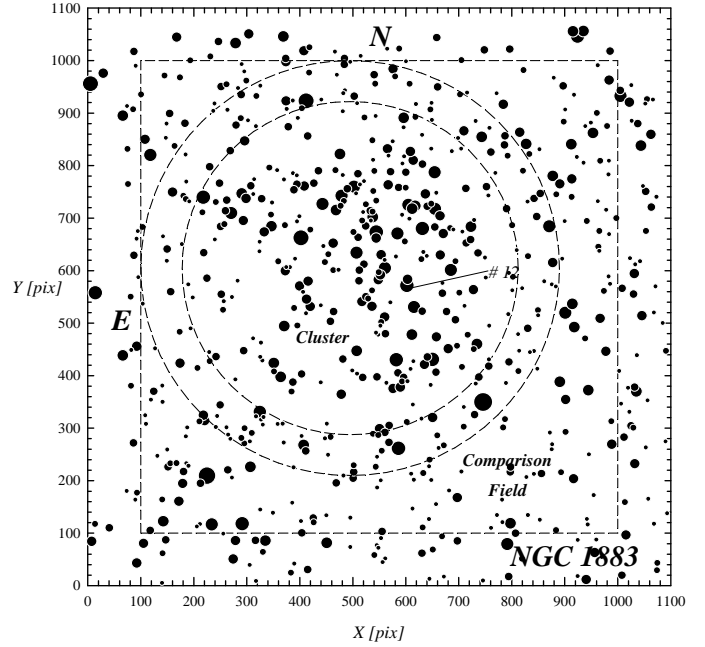


Figure 5. The field used for the Cluster Luminosity Function determination. The *Cluster Region* and the *Comparison Field* are indicated.

Table 3. Completeness results in NGC 1883.

V	%
10.5	100.0
11.5	100.0
12.5	99.9
13.5	99.5
14.5	97.3
15.5	96.1
16.5	95.8
17.5	90.1
18.5	73.4
19.5	62.0
20.5	41.3

in Fig. 6.

Here, the completeness, background corrected stars counts as a function of magnitude are shown together with their Poisson uncertainties. The LF is a rising function over the magnitude range for which our completeness is larger than 50%, except for the last bin, at V larger than 18. This seems to suggest that evaporation of low mass stars has been important during NGC 1883 evolution, in agreement with the findings in Sect. 8. Since this happens at the limit of our photometry, a deeper study is mandatory to make stronger our results.

We note in addition the presence of a statistically significant depression at $V \sim 15.5$, where also the MS in the CMD (see Fig. 1) does show a gap. Such gaps are common in open clusters, and a variety of explanations have been discussed over the years for their occurrence (Rachford & Canterna 2000).

Apparent magnitudes were then transformed into the absolute ones using the cluster apparent distance modulus (m-

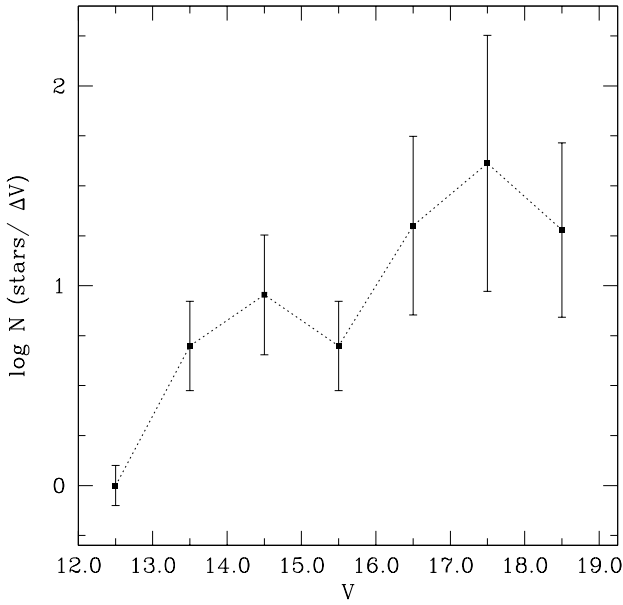


Figure 6. Cluster Luminosity Function.

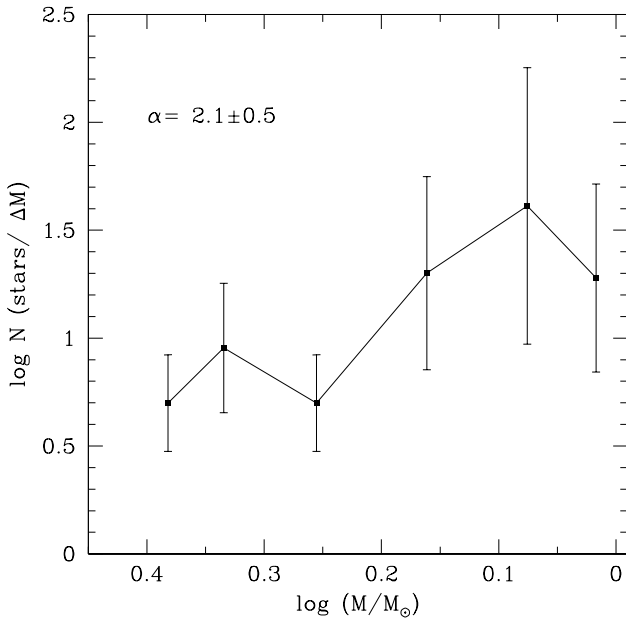


Figure 7. Cluster Mass Functions.

$M_V=14.3$. This allows us to compute the integrated absolute magnitude of the cluster by adding up star fluxes. We obtain $M_V = -2.4 \pm 0.2$. This value has to be considered as an upper limit, due to the possible presence of several field stars which we are not able to completely remove.

Finally the M_V distribution was converted into mass function (MF) using Girardi et al. (2001) theoretical models. The

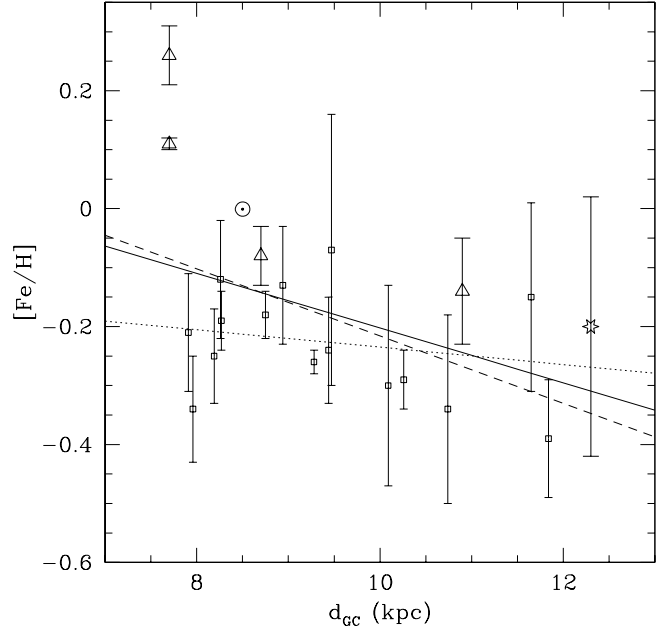


Figure 8. Galactic abundance gradient. Open squares are clusters from Friel et al. (2002), while open triangles are clusters found in the WEBDA database (see text for more details). The open star is the value for NGC 1883. The position of the Sun (8.5,0) is indicated

present day MF is shown in Fig. 7. A linear fit through the points yields 2.1 ± 0.5 for the α index, close to the Salpeter 2.35 value. As for the LF, we notice a deficiency of less massive stars, presumably due tidal mass loss. The integration of the present day MF gives a current total mass for NGC 1883 of about $240 M_\odot$, 3 times smaller than the mass at birth we derived in Sect. 7. This lend further support to a scenario in which substantial mass loss occurred as the cluster orbited the Milky Way.

10 DISCUSSION AND CONCLUSIONS

In Figure 8 we plot the Galactic radial abundance gradient as derived from Friel et al. (2002, hereafter F02) from spectroscopic observations of a sample of open clusters (open squares). We added also a sample of clusters not observed by F02 (open triangles). We selected these objects from the WEBDA database[§] with the condition of having metallicities spectroscopically determined to be homogeneous with F02 and with this paper. We plotted only clusters having age comparable with NGC 1883 ($0.5 \leq \text{Age} \leq 2.0$ Gyr, the same range used in F02 to identify the intermediate-age clusters sample). The whole sample defines an overall slope of -0.06 ± 0.01 dex/kpc (dashed line).

The open star represents NGC 1883, which follows the general trend very nicely. In fact, the continuous line, which

[§] WEBDA database on open clusters can be found at <http://www.univie.ac.at/webda/>

represents the radial abundance gradient determined by including also NGC 1883 basically coincides with the previous one, having a slope of -0.05 ± 0.01 dex/kpc. But we must notice that the slope is mainly driven by the two inner most metal rich open clusters (the inner triangles). If we exclude these points, the gradient is flat having a value of -0.01 ± 0.01 dex/kpc (the dotted line). Considering also the dispersion of the data and the error of the fit, we are led to the conclusion that Galactic gradient is flat, at least outside the solar circle. Inside it probably grows up to super-solar metallicity ($[\text{Fe}/\text{H}] \sim +0.2$). However this last point is not sure being based only on the metallicities of two clusters, and it needs further investigations.

On the other hand, as discussed by F02, the oldest open clusters ($\text{Age} > 4.0$ Gr) formed in our Galaxy demonstrate a strong gradient also outside the solar circle, as shown in Fig. 3 of F02. This is compatible with the scenario of a primordial pollution of the interstellar matter from which clusters were formed mainly in the inner regions of the Galaxy, following which the chemical enrichment was extended to the outer regions. The results was a present day homogenization of the chemical content in the Galactic disk giving a flat gradient as defined by the younger open clusters outside the solar circle. However this scenario is not valid for the outer regions of the Milky Way.

Carraro et al. (2004, hereafter C04), and Yong et al. (2005) found the presence in the outer disk of old open clusters ($\text{Age} > 4$ Gyr) having a metallicity of about -0.5 dex, well above the value of the gradient as defined by the inner old clusters. This means that probably the outer disk had a peculiar chemical evolution, probably driven by the contamination of external objects (dwarf galaxies) cannibalized by the Milky.

On the other hand only few intermediate-age clusters were observed for metallicity determination in the outer disk at medium-high resolution, the majority of them being located close to the Sun.

The addition of NGC 1883 indicates that the gradients keep flat for half a kpc more, suggesting a trend which further studies can possibly confirm.

We finally note that the gradient exhibits quite a significant scatter. One may wonder whether this solely depends on observational errors, or whether this scatter reflects a true chemical inhomogeneity in the Galactic disk.

Further observations are needed, especially in the not well explored Galactic region between 14 and 22 kpc from the Galactic center. We are actually engaged in such exploration, with new results being presented in Carraro et al. (2007, submitted to AJ).

ACKNOWLEDGEMENTS

This paper is based on data collected at the Mount Ekar Observatory, Asiago (Italy). We wish to express our gratitude to the technical staff of the Observatory. In our investigation we made use of WEBDA. Finally, the authors wish to thank the referee, Bruce Carney, for useful comments.

REFERENCES

- Alonso, A., Arribas, S. & Martínez-Roger, C. 1999, *A&AS*, 140, 261
- Barmina, R., Girardi, L. & Chiosi, C. 2002, *A&A*, 385, 847
- Baume, G., Vázquez, R. A. & Carraro, G. 2004, *MNRAS*, 355, 475
- Baume, G., Carraro, G., Costa, E., Méndez, R.A., Girardi, L., 2007, *MNRAS*, 375, 1077
- Carraro, G. & Chiosi, C. 1994, *A&A*, 287, 761
- Carraro, G., Baume, G. & Villanova, S. 2003, *MNRAS*, 343, 547
- Carraro, G., Bresolin, F., Villanova, S., Matteucci, F., Patat & F., Romaniello, M. 2004, *AJ*, 128, 1676
- Carraro, G., Subramaniam, A., Janes, K.A. 2006, *MNRAS*, 371, 1301
- Cescutti, G., Matteucci, F., François, P. & Chiappini, C. 2007, *A&A*, 462, 943
- Chabrier, G. 2001, *ApJ*, 554, 1274
- Dias, W. S., Alessi, B. S., Moitinho, A. & Lépine, J. R. D. 2002, *A&A*, 389, 871
- Elson, R. A. W., Sigurdsson, S., Davies, M., Hurley, J. & Gilmore, G. 1998, *MNRAS*, 300, 857
- Friel, E. D. 1995, *ARA&A*, 33, 381
- Friel, E. D., Janes, K. A., Tavares, M., Scott, J., Katsanis, R., Lotz, J., Hong, L. & Miller, N. 2002, *AJ*, 124, 2693
- Girardi, L., Bressan, A., Bertelli, G. & Chiosi, C. 2000, *A&AS*, 141 371
- Girardi, L., Groenewegen, M. A. T., Hatziminaoglou, E. & da Costa, L. 2005, *A&A*, 436, 895
- Groenewegen, M. A. T. & Salaris, M. 2001, *A&A*, 366, 752
- Houdashelt, M. L., Bell, R. A. & Sweigart, A. V. 2000, *AJ*, 119, 1448
- King, I. 1962, *AJ* 67, 471
- Kroupa, P. 2001, *MNRAS*, 322, 231
- Lamers, H. J. G. L. M., Gieles, M., Bastian, N., Baumgardt, H., Kharchenko, N. V. & Portegies Zwart, S. 2005, *A&A*, 441, 117
- Kurucz, R. L. 1992, in *IAU Symp.* 149, *The Stellar Populations of Galaxies*, ed. B. Barbuy & A. Renzini (Dordrecht: Kluwer), 225
- Phelps, R. L., Janes, K. A. 1994, & Montgomery, K. A. 1994, *AJ*, 107, 1079
- Piskunov, A. E., Schilbach, E., Kharchenko, N. V., Rser, S. & Scholz, R. D. 2007, *astro-ph/0702517*
- Rachford, B.J., Canerna, R. 2000, *AJ*, 119, 1296
- Schlegel, D. J., Finkbeiner, D. P., & Davis, M. 1998, *ApJ*, 500, 525
- Tadross, A. L. 2005, *BASI*, 33, 421
- Tiede, G. P., Martini, P., & Frogel, J. A. 1997, *AJ*, 114, 694
- Twarog, B. A., Ashman, K. M. & Anthony-Twarog, B. J. 1997, *AJ*, 114, 2556
- Vallenari, A., Carraro, G., Richichi, A. 2000, *A&A* 353, 147
- Yong, D., Carney, B. W., Teixeira de Almeida, M. L. 2005, *AJ*, 130, 597